SENSOR LETTERS
Vol. 6, 1–13, 2008

The Use of PE/PVDF Pressure and Temperature Sensors in Smart Wireless Sensor Network System Developed for Environmental Monitoring

Essa Jafer* and Khalil Arshak

Electronic and Computer Engineering Department, University of Limerick, Limerick, Ireland

(Received: 7 May 2007. Accepted: 5 May 2008)

In this work, a design of wireless system for multi-sensors monitoring has been presented. The main purpose of this research is to develop an efficient telemetry system for measuring water pressure and temperature signals. The system reads data from two types of sensors, temperature (resistive) and pressure (capacitive). Anderson circuit configuration has been used for the resistive sensor, since it offers linear like behavior. The capacitive interface is based on capacitance-frequency-voltage conversion that uses phase lock loop to convert the frequency to voltage. A developed pressure sensors based on polyethylene and polyvinylidene fluoride, were used to evaluate the performance of the capacitive interface. A small size wireless module has been built separately to test the capacitive interface for a certain range of pressure. Two mechanisms have been adopted to reduce the overall power consumption. These are power scheduling and wakeup circuit for the capacitive interface. The first one is implemented fully by the micro-controller unit (MCU) in order to switch on/off all the system units. A wakeup circuit has been designed to interrupt the MCU when it is in the sleep mode and the capacitive samples are changing significantly. A platform for wireless sensor network (WSN) has been developed so that the receiver side can communicate with more than one sensor node.

Keywords: Wireless Sensor Network (WSN), Environment Monitoring, Pressure and Temperature Sensors, Capacitive and Resistive Interfaces.

RESEARCH ARTICLE

1. INTRODUCTION

There is a considerable interest in the development of multi-sensor micro-systems for use in the implanted,[1,2] ingestible[3,4] and remote environmental monitoring.[5] Building a complete sensor micro-system involves several challenges as these designs include not only a union of the analog and digital circuit domains, but also the magnetic, mechanical, biological, chemical, or electrical domains. Such systems must exhibit low-cost production, robustness of use and real-time data processing.

Many sensor micro-systems have been proposed and implemented recently. In Ref. [6], a typical low power sensor interface smart micro-system has been presented. The system consumes low power and is compatible with a wide range of capacitive transducers. Similar micro-system that incorporates different sensor interfaces is described in Ref. [7].

*Corresponding author; E-mail: essa.jafer@ul.ie

In the field of environment monitoring, a number of systems have been developed and applied. A wireless sensor module for recording different ambient conditions like temperature and humidity is presented in Ref. [8]. Such system uses high rate RF transceiver and field programmable gate array (FPGA) to implement digital signal processing (DSP) tasks. Another wireless remote environment monitoring system is presented in Ref. [9], where the MCU is operating in sleep and wakeup modes to reduce power consumption. In Ref. [10], a system is introduced that utilizes inductive power and data transfer through a backscatter-modulated carrier and a transducer interface that monitors its environment through embedded capacitive transducers is introduced.

Measuring the water pressure and temperature under different conditions is still important to be determined. For examples, many systems have been presented in the past to sense the water pressure under the sea and the ground.[11,12] Recently wireless technology became attractive for remote

monitoring where the data recorded by different sensors can be recorded and sent to a Base Station for analyzing.[13] Due to this, we developed a new wireless smart system for localized monitoring of both temperature and pressure in real time by means of centralized wireless receiver. The work in this paper focused mainly on the development of pressure sensors and the design of an efficient power management for the transmitter side of the system.

2. SYSTEM ARCHITECTURE

Figure 1 shows the system overview diagram. The word mote is used here as a short term for describing the wireless remote sensor. Based on the commands sent by the Base Station, the mote is configured to be for either resistive or capacitive measurements. The output samples from the signal conditioning circuit will be processed and buffered by a microcontroller before the transmitter becomes ready. The data will be sent to the Base Station over 433 MHz channel using Frequency Shift Keying (FSK) modulation type. The mote also has the ability to power off the appropriate conditioning interfaces if they are not being used or between the sampling times of the two analog signals to save power.[14] The bi-directional wireless communication will be responsible to direct the mote system by sending suitable commands and on the other hand receive the recorded sensor data. The remote controlling station can select the type of sensor data need to be sent, either pressure or temperature and command the mote to switch off the unused sensor interface. In addition the Base Station can adapt the settings of the mote power management and sampling frequency based on the nature of the data received. Such feature has proven to be very advantageous for any smart system[15] to overcome uncertainties.

The Base Station is able to communicate with multiple motes. This can be accomplished by using a form of time-division multiplexing (TDM), where the Base Station coordinates for each mote to start transmission. Such protocol has been proved to be an efficient way of gathering data from number of nodes into one wireless channel.[16] The proposed TDM protocol assigns a time slot for each active channel after polling all the existed motes. A distinguish header is associated with each data frame so that the Base Station can tell which channel is which. To reduce the cost of this overhead, only a few characters for each channel are grouped together for transmission.

The data received from all motes at the Base Station are then sent to a PC via RS232 serial communication. A general purposes PIC microcontroller has been used in both sides of the systems. The MCU has internal analog to digital converter (ADC) and Universal Asynchronous Receiver Transmitter (UART) for testing and interfacing with a PC. The mote is operating using 3.3 V lithium battery that has a very high energy density and offers a longer battery life. The Base Station is powered using 9 V AC-DC power supply and has a backup battery for operation when power is shut down suddenly.

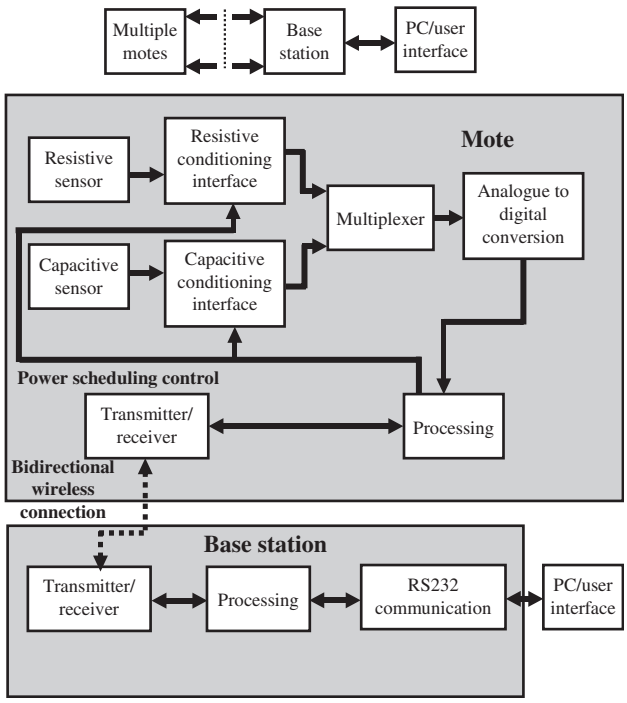

Fig. 1. System overview.

3. SENSOR DEVELOPMENT AND MANUFACTURING

In this study, capacitive pressure sensors were fabricated using sandwich structure.[17, 18] DuPont 4929 silver conductive paste was used to form the electrodes which were printed onto alumina and Melinex® substrates using a DEK RS 1202 automatic screen-printer as shown in Figure 2. After printing, the substrates were allowed to cure at 120 °C for 30 minutes. A Thelco Model 6 oven was used for this purpose.

3.1. Sensor Testing Mechanisms

After fabrication, the sensors on alumina substrates were placed in a cantilever beam arrangement so that the change

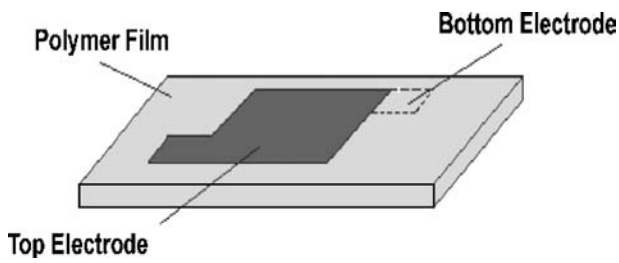

Fig. 2. Shows the structure of the PVDF and PE capacitor.

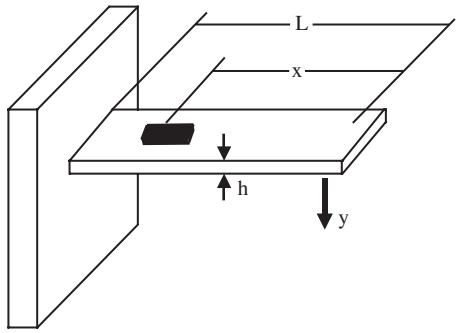

Fig. 3. The cantilever beam arrangement.

in capacitance with applied strain could be measured. The experimental arrangement is shown in Figure 3. It can be seen from Eq. (1) that with knowledge of the beam geometry and displacement, the strain on the sensor can be calculated.[17]

$$\varepsilon = \frac{3xyh}{2L^3} \tag{1}$$

Where ε is the strain, x is the distance from the centre of the beam to the point where the load is applied, y is the displacement of the beam and L is the distance from the clamped end to the point where the load is applied. By measuring the change in capacitance, ΔC and the applied strain, the gauge factor (GF) can be calculated from Eq. (2), where C is the original, or base line capacitance. The change in capacitance GF was measured using a HP 4192A LF Impedance Analyzer.[17]

$$GF = \frac{\Delta C/C}{\varepsilon} \tag{2}$$

3.2. Sensor Development

The two materials polyethylene (PE) and polyvinylidene fluoride (PVDF) were chosen for their biocompatible and mechanical properties. Capacitive structures are preferred as they lead to lower power consumption and higher sensitivity than their piezoelectric counterparts.[19]

PVDF is a low-density semi-crystalline material, consisting of long repeating chains of -CF_2-CH_2- molecules. The crystalline region consists of a number of polymorphs, of which the α- and β-phase are most common. The β-phase is piezoelectric and has many advantages including its mechanical strength, wide dynamic range, flexibility and ease of fabrication.[20, 21] Poled PVDF films have been employed in the development of devices, which can be used in a wide range of applications, for example, providing robots with tactile sensors and the measurement of explosive forces.[22, 23]

In a medical context, poled PVDF films have been popular in the development of planar pressure-measurement systems, where their flexibility and the ease with which electrode patterns can be attached has been a particular advantage. Micromachined devices using PVDF as a flexible element in the system have also been developed for use in an endoscopic grasper because of its high force sensitivity, large dynamic range and good linearity.[24]

Polyethylene is a cost effective and versatile semi-crystalline polymer consisting of repeating -CH_2-CH_2- units. The most common forms are low-density polyethylene (LDPE) and high-density polyethylene (HDPE), where the density is related to the degree of chain branching. It is a material which is useful in pressure sensing applications and has been popular for use in the development of flexible electronics.[25] PE is particularly popular in the fabrication of polymer/carbon-black composites for pressure measurement.[26] Furthermore, polyethylene terephtalate (PET) has been identified as an electret material with possible dynamic pressure sensing applications.[27]

In this work, both PE and PVDF films were formed into a sandwich capacitor, which was then subjected to changing hydrostatic pressures. The films deformed under pressure and the resulting change in capacitance was transmitted wirelessly through the liquid to an external receiver, which converts the signal to a corresponding voltage.

3.3. Experimental Procedure

When parallel plate capacitors, such as those formed in this study, are placed under pressure, the thickness of the sensing layer changes, resulting in an alteration of the distance, d, between the electrodes or plates. When the pressure is applied uniformly, there is a correspondingly uniform change in d, which leads to a change in the overall capacitance, according to Eq. (3).[19]

$$C = \frac{\varepsilon_r \varepsilon_o A}{d} \tag{3}$$

where, C is the capacitance, ε_r, is the relative permittivity of the dielectric, ε_o is the permittivity of free space and A is the area of the capacitor plates. The capacitance was found to be 40 pF and 140 pF for the PE and PVDF sensors respectively. The relative permittivity was measured to be 3.45 for PE and 9.27 for PVDF at a frequency of 1 MHz. The frequency response of the two sensors has been measured using the Impedance Analyzer. Both materials showed a high stability over a wide range of frequencies, as shown in Figure 4, making them well suited for integration into the wireless data acquisition system.

The above behavior is due to the low dielectric absorption of the two materials which causes the C value not significantly changing. Equation (4) describes the relation between the C value and the dielectric loss:[28]

$$C(f) = C_o\left[\left(j\frac{f}{f_o}\right)^k\right] \tag{4}$$

Where C_o is the capacitance at particular frequency f_o

K is negative constant that set the rate of deterioration in C per decade which represents the loss tangent value.

RESEARCH ARTICLE

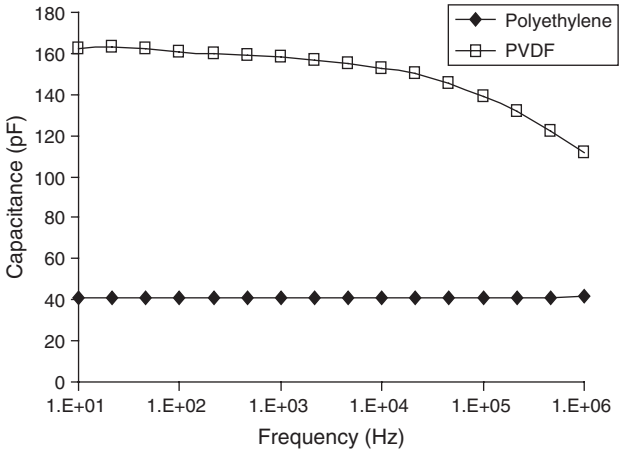

Fig. 4. Variation of capacitance with frequency for PE and PVDF devices.

As frequency goes higher C is expected to go down at a certain frequency range based on the dielectric constant of the sensor.

4. DEVELOPMENT AND TESTING OF WIRELESS CAPACITIVE MODULE

A wireless data acquisition system, including a capacitance to frequency converter (C/F) and an internal voltage regulator to provide a stable operation has been developed as shown in Figure 5. At the receiver side, CD4046 phase locked loop (PLL) unit is used to convert the received frequency to voltage which is more stable. The TLC556 dual CMOS timer (manufactured by Texas Instrument)[29] is used in astable configuration to generate a square wave signal with approximately 50% duty cycle. The system was developed specifically for testing the performance of the capacitive sensors.[30]

The wireless sensor module has been accommodated by a square water proof box of a size (length × width × height) $59 \times 54 \times 30$ mm^3 as shown in Figure 6. The sensor has been mounted on the top of the box through a sealed hole to sense the omni-directional pressure exerted by the water.

The used test bench is consisted of a tube that has been filled with water as shown in Figure 7. For each sample test, the box is attached to certain weight that push it down

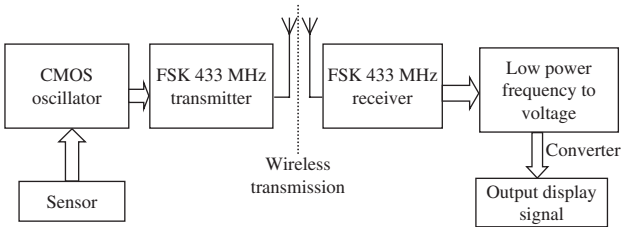

Fig. 5. Block diagram of the interface, transmitter and receiver system used to make measurements under hydrostatic pressure.

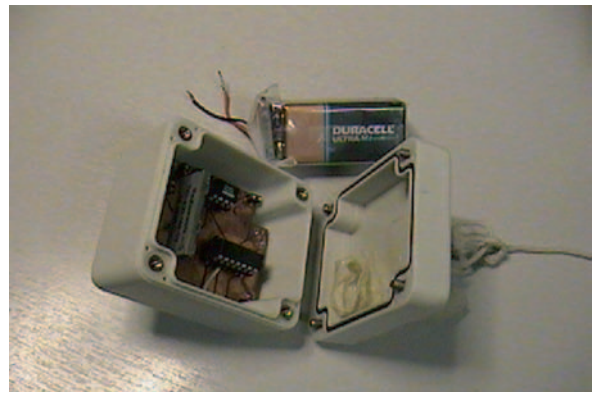

Fig. 6.

to the bottom of the tube which causes a uniform pressure changes determined by the height which has been calculated in prior to cover the required pressure range.

Figure 8 shows the response of the PE and PVDF sensors to pressure in the range 0–17 kPa. The change in voltage was recorded by the wireless module and sent through an RF link to the receiver. The details of the capacitive interface circuitry, which is based on C-F-V conversion, are given in the next section.

It was observed that PE shows a higher sensitivity to pressure changes than the PVDF film. The change in voltage is related to the capacitance change, which is a direct result of deformation of the dielectric layer under pressure. For the PE sensor, the voltage changes by 20 mV over the entire range. For the PVDF sensor the change is 5 mV. It can be seen from the results that PE sensors show the highest sensitivity, and are well suited to pressure measurement over the range tested. On the other hand PVDF devices may be more useful for measurements over larger ranges.

Each device was also subjected to a repeated cycling, in order to establish its repeatability (the maximum difference between output readings as determined by two calibrating cycles). Five cycles are shown for PE in Figure 9(a) and PVDF in Figure 9(b). The repeatability was calculated to be 10% and 6% for PE and PVDF respectively. This can

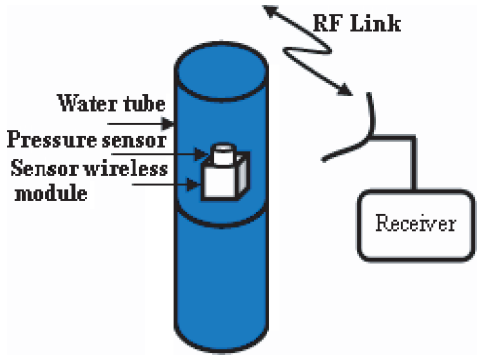

Fig. 7. Block diagram of the developed test bench for the capacitive wireless sensor.

RESEARCH ARTICLE

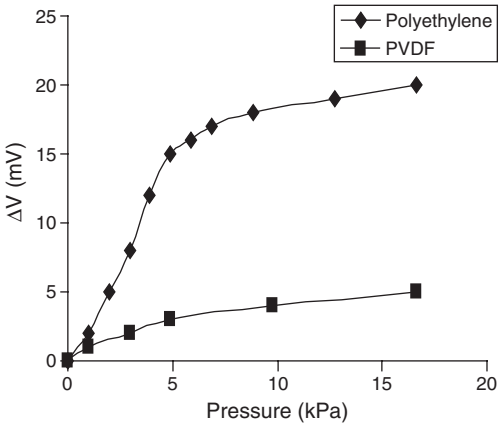

Fig. 8. Change in voltage with pressure in the range 0–17 kPa for the PE and PVDF sensors.

be attributed to movement of the polymer chains while they are under pressure.[31] The more rigid nature of the PVDF results in lower percentage repeatability, as it does not suffer the same degree of slippage.

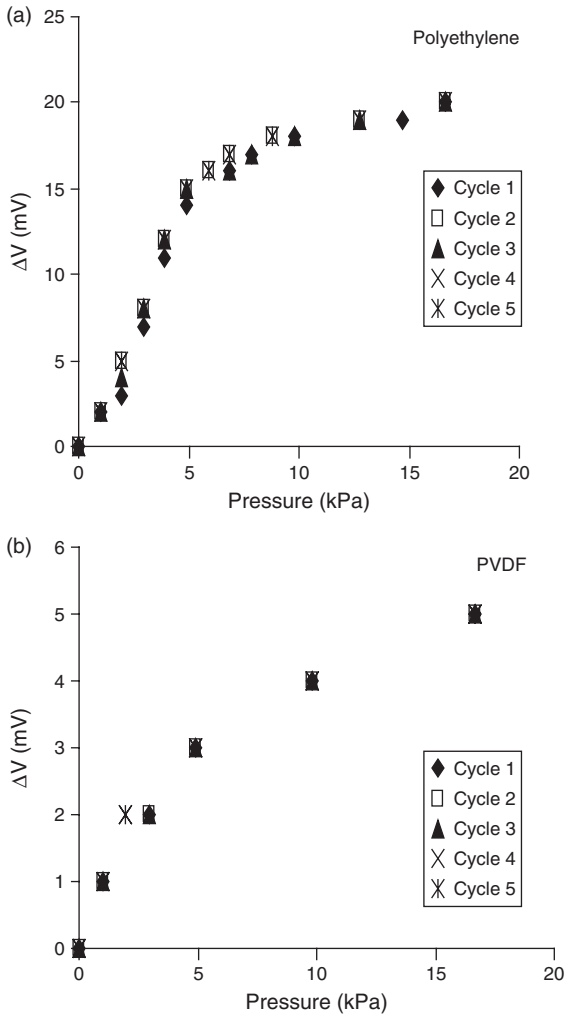

Fig. 9. Repeatability of (a) the PE sensor and (b) the PVDF sensor as measured for five loading cycles.

5. DESIGN OF THE SMART WIRELESS SYSTEM

In this section, the design options for both resistive, capacitive signal conditioning circuits and power management are presented:

5.1. Microcontrollers

The family of Microchip PIC18Fx2 processors has many peripheral features that are useful in our application, while still drawing relatively small amounts of current (for example, approximately 5 mA at 20 MHz). The PIC18LF452 microcontroller (MCU) was selected for use on both the Mote and Base Station. Some of the I/O features are common to both sides of the application, while others are specific to the unit. These features and functions are described in the following section.

5.2. Mote Microcontroller

For our design, the selection of either a microcontroller or general purpose microprocessor will affect the functionalities of the product and the complexity of the system greatly. Since most of the general purpose microprocessors require more peripheral ICs in order to perform similar functions that would be provided by a generic microcontroller, the amount of additional ICs will result in greater power consumption. Therefore, a general purpose microprocessor is eliminated for this design.

Although PIC microcontroller families provide a wide range of selections, it is still necessary for additional criteria to be set in order to select a MCU that is the best fit for this project. The criteria in Table I list the requirements which were set in a value that has weight from 1 to 5. These values indicate the priorities of selecting 9 features of the microcontroller to suit the given requirements.

In order to program in *C* to simplify the complexity of coding, a well developed programming environment is essential for the design. Freely, microchip provides and supports a compiler, *C*18 to complete this task; however, the compiled code size became an apparent issue for coding in the *C* environment. Therefore, the size of programming memory and random access memory are also

Table I. Mote microcontroller selection criteria.

Requirement	Weight
ADC	2
TX(transmitter)/RX(receiver)	1
Data memory (RAM + EEPROM)	4
Sleep support	4
Interrupt source number	1
Flash program memory size	3
Program environment	5
No of available GPIO	4
Hardware I2C/SPI support	3

RESEARCH ARTICLE

included with heavier weights. Lastly, the support of SPI and I2C in hardware greatly reduces troubles such as shortage of processing cycles that could be raised from using software emulated I2C and SPI.

After the criteria were deduced within the PIC MCU families, three PIC microcontrollers have been considered based on the design options given in Table I, these are PIC16F877, PIC18F452 and rfPIC12C509AF.[32]

The rfPIC12C509AF belongs to the rfPIC family that aims to provide on chip transceiver ability to meet the increasing demand of RF products. However, it has a very small programming memory size, in which only the required protocol can be fit. In our Mote design, a much larger code size is required not only because of the limitations of the *C* compiler, but also because of the data acquisition functions that the product aims to provide. Therefore, rfPIC12C509Af is also eliminated from the choices. The differences between the 16F family and the 18F family are not very distinctive besides higher processing speed and larger program size. In order to make sure that there is enough buffer memory for the sampling data, the PIC18F452 is selected as the best MCU for the mote.

5.3. Base Station Microcontroller

For the Microcontroller on the Base Station, the requirements were similar to those of the Mote in several points. The difference between the requirements of the Base Station and the Mote are that the Base Station does not require an ADC or low-power operation, while it does require some form of support for an RTC (Real Time Clock), and RS232 communication.

5.4. Transceivers

The wireless aspect of the design was achieved using an off-the-shelf transceiver with 433 MHz band using FSK (frequency shift keying) modulation. The ChipCon[33] transceiver plug and play module CC1000PP is the optimised evaluation board for the single chip transceiver, CC1000. This chip features low power and completely configurable under the control of software for many frequency bands, signal strengths, and has support for frequency hopping.

The evaluation module is built with all the necessary passive components required for operation. The module is 28 mm by 20 mm with jumper terminals for fast prototyping. Therefore all external connections to the module are placed on the two jumper terminals. The supply voltage for the plug and play board is between 2.1 and 3.6 V and the filter is pre-mounted on the board.

5.5. Wireless Communication Protocol

The wireless smart system relies on a prefabricated transceiver unit operated at frequency 433 MHz. Both FSK and Manchester encoding are employed by the unit at a maximum speed of 38.4 Kb/s. The transceiver is half-duplex, however switching between the two ways of transmission can be done quickly. Devices that are not actively transmitting should be either in receive or polling mode depending on the power restrictions of the device.

Several protocol standards were investigated as a possible alternative to designing a new protocol.[34, 35] The standards found are mostly used in remote sensing and building/home automation and control. The following criteria were used as a guideline for comparing the protocols:

- Multiple Node Support:
  - Bi-directional Communication
  - Addressing—Each node in the network be addressed individually.
- Efficiency:
  - Overhead—Number of headers must be added to data packets.
  - Complexity—Higher protocol complexity means more processor cycles needed to send a message
- Transmission Control–support of:
  - Error-Detecting/Correcting Codes
  - Collision Detection
  - Message Queuing
- Availability of:
  - Protocol Standards
  - Sample Source Code

It was found that most of the standard protocols are all well suited in the areas listed above; however there are some drawbacks. These are either a subset of the protocol is required, which makes the use of it not justified, or it is complex to be employed in the design. As a result of these concerns with each of these protocols, it was decided that it would be best to develop a custom-written protocol; this way it can be custom-tailored to meet the needs of this application.

The data link layer encapsulates the data blocks to be transmitted in a frame structure or a packet. The protocol developed for this purpose is bit-oriented where bytes are always transmitted with their most significant bit (MSB) first. The general frame structure is shown in Figure 10, with the size of each field. The command field is used to indicate the nature of the transmission. It is generally one

Start (1)	Length (1)	Mote address (2)	Base address (1)	Command (1)	Date (1–250)	Checksum (1)

Fig. 10. General packet structure.

byte, followed by variable or fixed-length data. The header check sum is 8-bit sum of the data packet bytes.

5.6. Resistive Interface

Anderson Loop[36] circuit topology has been selected for the resistive interface circuitry. In this configuration, a practical dual-differential subtractor with sufficiently high input impedance and rejection of unwanted signals has been introduced as shown in Figure 11. Here voltage drops along current-carrying lead wires, Z_{w1} and Z_{w2} are simply not included in the signals being processed. No significant voltage drop occurs along the sensing lead-wires, Z_{w3} and Z_{w4}. When the reference impedance, Z_{ref} is chosen to be equal to the initial impedance Z_g, of sensing element, the subtractor inputs are processed with unity gain and the output will be:[36]

$$\nu_{out} = i\Delta Z \quad (5)$$

Where i is the circuit bias current. The results indicate that the loop has an inherently linear response to changes in a sensor element and no impedance terms are present to attenuate the output.

The diagram for resistive interface circuit is shown in Figure 12. The design is implemented to be configurable for various measurement ranges by selecting appropriate values for R_{bias}, R_{ref} and instrumentation amplifier gain control resistors R_{G1}, and R_{G2}.

The schematic of the developed resistive circuitry is shown in Figure 12. For the constant current excitation, a voltage regulator is used to get a precision voltage drop R_{bias}. This creates the bias current for the current mirror, which is composed of two NPN Bipolar Junction Transistors (2N3904). In this way, the current entering the collector of Q1 is also induced at the collector of Q2. However, the current can vary for a particular transistor with temperature fluctuations. To overcome this, the transistors

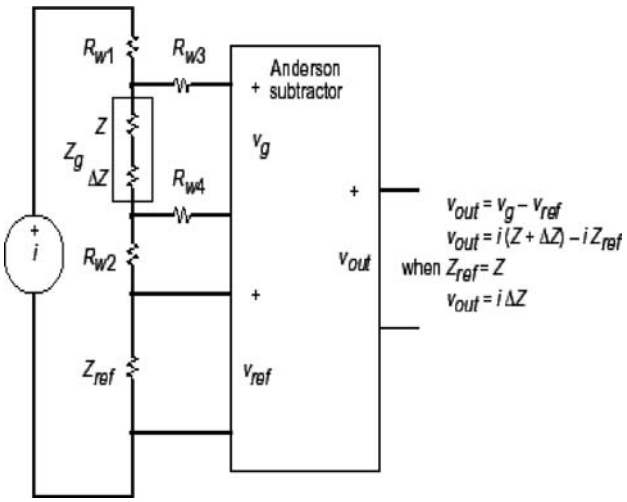

Fig. 11. The Anderson loop measurement circuit topology.

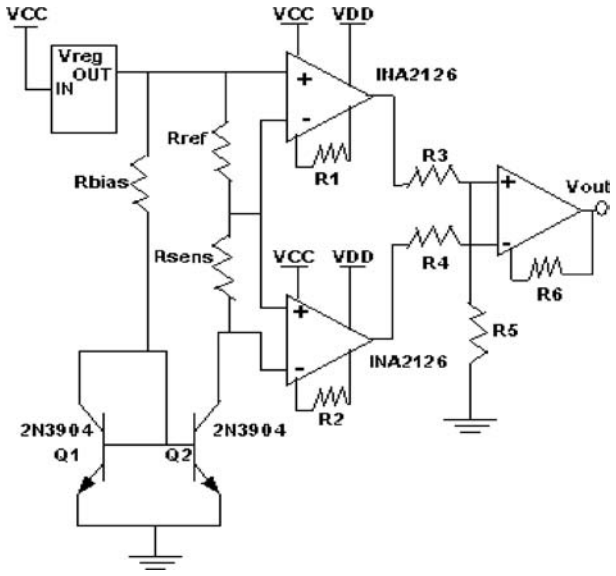

Fig. 12. Resistive interface circuitry schematic.

are joined together using epoxy to ensure getting stable current.

5.7. Capacitive Interface

Based on the output of testing the capacitive interface, it was found that the sent frequency tones might be drifted due to the effects of the wireless medium. According to this, it has been decided to convert the frequency to voltage and use the MCU in the mote to convert it to digital information before sending it wirelessly. Another

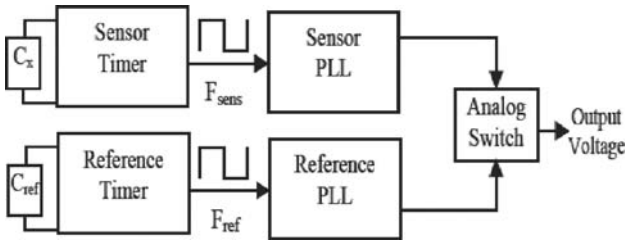

Fig. 13. Block diagram of the capacitive circuitry in the mote system.

Table II. Power consumption compression for different capacitive sensor interface circuits.

Interface	Current consumption	Supply voltage (minimum)
Universal capacitive readout IC-MS3310[38]	2.9 to 6.0 mA	5 V
AC bridge (simulated)	2 to 10 mA	None
Anderson loop[36] (implemented)	1 to 3 mA	3 V
C-F-V, (using *F-V* converter) LM2907 (implemented)	5 to 8 mA	3 V
C-F-V, (using *F-V* converter) TC9400 (implemented)	1.5 to 6 mA	10 V
C-F-V, PLL (implemented)	<500 μA	2.3 V

RESEARCH ARTICLE

reference capacitor will be used for calibration as shown in Figure 13. The PLL circuit was found to be more adequate and has a higher sensitivity for changes in the desired capacitance range. In Ref. [37] the parameters of the PLL design were discussed in great detail.

In addition the PLL circuit was found to have lower power consumption when compared to standard frequency-to-voltage converter configurations and other interface circuits as clarified in Table II.

6. SYSTEM POWER MANAGEMENT

Since it is required to reduce power consumption on the mote as much as possible, Power scheduling has been designed carefully to control the different parts of the system. Figure 14 shows the power flow mechanism which is mainly controlled by the processor unit. The transceiver and MCU have a "sleep" mode that can be controlled from the software.

As shown above, the sensor signal conditioning circuits can be switched on or off by the control signals of the processor unit. A CMOS analog switch is used for this purpose. Table III clarifies the power scheduling options for the sensor interface circuits. In order to preserve the power, certain modules within the mote system are powered off when they are not in use.

At any one time, mote system is configured to read either resistive or capacitive samples. For the resistive interface, mote is powering on/off for each sample (max sampling rate 200 samples/sec). The capacitive interface is powered from a 2 V supply which is less than that for the resistive and has a large start-up time of about 200 ms.

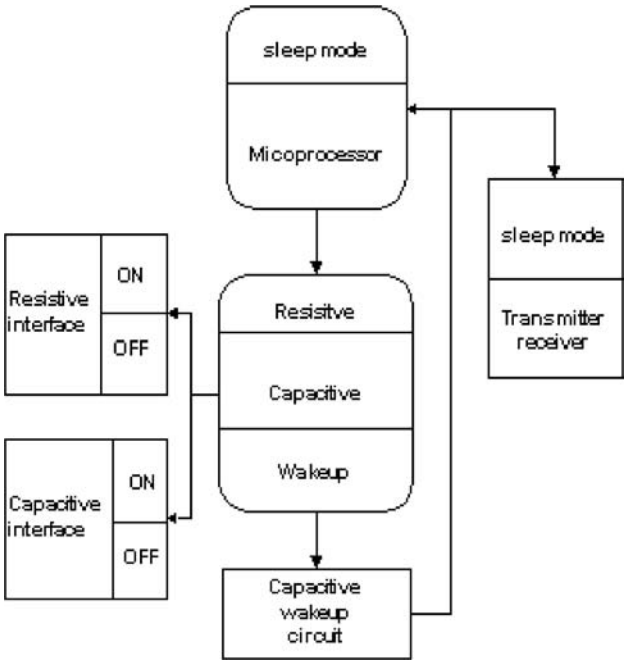

Fig. 14. Power control of the mote system.

Table III. Sensors interfaces power scheduling.

μP	Resistive	Capacitive	Wakeup
Wakeup	ON	OFF	OFF
Wakeup	OFF	ON	OFF
Sleep	OFF	OFF	ON

On the other hand, resistive interface consumes high current (15 mA) and has a low start-up time (~1 ms). This makes it infeasible to be turned on/off the capacitive unit for each sample since it draws already a very low current (~400 μA). As a result, the capacitive interface will be left on constantly when being used.

For further power consumption reduction, a wakeup circuit, which allows the processor to enter sleep mode while capacitive readings are not changing, has been developed. It has been noticed that wakeup circuit is not suited for the resistive interface where a higher power is needed to keep the circuit operating constantly. The wakeup circuit must be on when the capacitive sensor is being used and the processor unit is in sleep mode. The wakeup circuit is turned off either when the capacitive is being used and the processor is on, or when the resistive is being used.

6.1. Wakeup Circuit Design

The purpose of the wakeup circuit is to put the MCU in sleep mode when the input signal is not changing. When the signal starts to give a significant change, an interrupt is generated that wakes up the MCU and it will start sampling again. The circuit is designed as shown in Figure 15.

The design is based on the principle of window detector, where two digitally controlled potentiometers are used to set the upper and lower trip points of the two comparators. At the beginning of operation, the MCU decides when the capacitive samples are not changing, and then it will set the upper and lower limits of the window and powers up the wakeup circuit. The MCU will be in sleep mode when the sensor goes outside the limit. Than an interrupt signal will be generated to wakeup the MCU that will power down the wakeup circuit to save power.

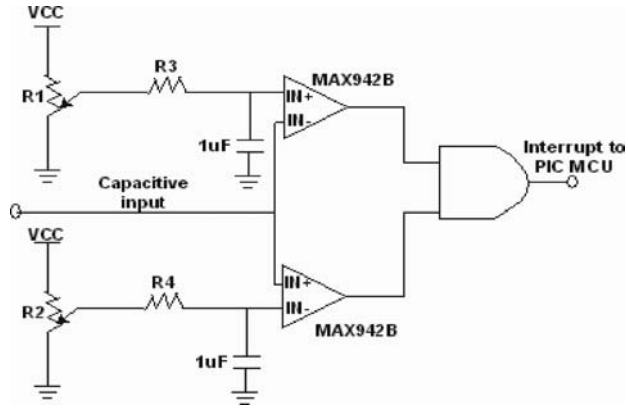

Fig. 15. Wakeup circuit diagram.

RESEARCH ARTICLE

The above design draws about 700 μA, and the interrupt signal will be generated by a NAND gate that outputs zero when the sensor is within the window range. If the sensor goes above the upper-trip or below the lower trip, the desired output is high, that will interrupt the MCU from the sleep mode.

6.2. Base Station Backup Power System

The Base Station is powered using 9 V AC-DC wall power supply. In case the wall power is failed for any reason, a battery backup circuit has been designed to provide an alternative voltage source for a reasonable time period.

The Base Station requires different voltage levels to operate. Since it was planned to operate the digital system from a 3 V voltage level, and the RS232 communications requires higher voltage levels (for example the series of Maxim MAX232 require 5 V), it was decided to use two voltage regulators, one 3 V and one 5 V. The voltage regulators that were selected are Texas Instruments TPS72-series ICs.[39]

Figure 16 shows the Base Station power system schematic, complete with battery backup functionality. When the 9 V supply is functioning properly, the input to the 5 V regulator is approximately 8.3 V, after the 0.7 V drop across D1. In this state, D2 is reverse biased and no current flows from the backup battery. If the wall supply drops out, D2 becomes forward biased and current flows from the backup battery. C1 helps to hold the power constant during transitions from wall to battery power, and vice versa.

R1, R2, R3, D3, D4, and the MAX942 comparator provide a signal to the microprocessor when the backup battery is being used. D3 and D4 provide a combined drop of about 1.4 V from the 5 V supply, and R3 acts as a current-limiting resistor. Since the comparator must output a positive logic level of 3 V (max), it is driven off of the 3 V supply. As a result, the inputs cannot go above 3 V, and a voltage divider is used to protect the MAX942. When the

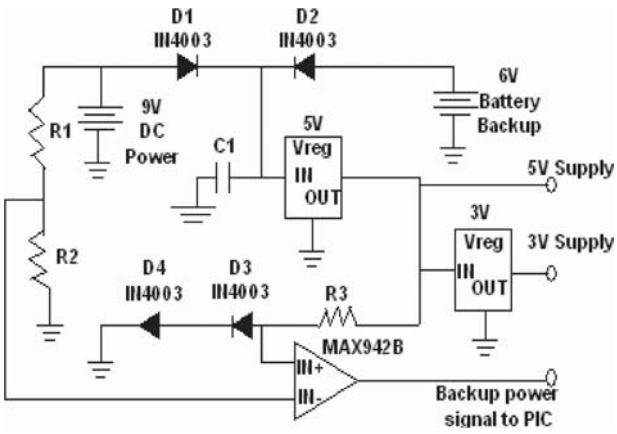

Fig. 16. Base station power system schematic.

Table IV. Current consumption specifications of the mote system.

Mote part	Current value	Units	Duty cycle %
Transceiver sleep mode	0.5	μA	
Transmitter current	10 (at 10 dBm)	mA	6.56
Receiver	8	mA	5
Resistive circuitry	1.5	mA	20
Capacitive circuitry	400	μA	100
Wakeup circuit	0.7	mA	100
MCU current	3	mA	100
MCU sleep current	16	μA	

9 V supply is present, R1 and R2 form a voltage divider that feeds approximately a 2.25 V into the negative terminal of the comparator. This also protects the comparator from DC wall spikes as high as 12 V. If the 9 V supply drops out, the positive terminal becomes the higher voltage terminal, and the comparator outputs a positive logic level informing that the Base Station is now running off of the backup battery.

6.3. Power Usage

Table IV summarizes the current consumptions of the different mote system units and their working duty cycles. It is clear from the table that most of the power is consumed by the sensors signal conditioning circuits and the transceiver. It can be noticed that the wakeup circuit draws higher current ($\sim$0.7 mA) when it is ON than the capacitive interface when it is working. However the capacitive with the wakeup circuit still draw less current than the MCU. The maximum efficiency can be reached with the capacitive when the signal does not change considerably over time.

7. RESULTS AND DISCUSSION

7.1. Sensors Measurements

The double sided PCB technology has been used to develop both systems. The overall size of the final mote top board is 30×33 mm^2. The mote has been placed in the developed test bench and interfaced to pressure and temperature sensors. A commercial temperature sensor from ANDIGILOG[40] has been used for this purpose to examine the performance of the resistive interface circuitry since it consumes a very little power with high-precision and miniaturized size. The two sensors are exposed to the water through two holes drilled on the top of the water proof box and covered by a flexible material to prevent water leak. The amount of pressure attenuation caused by this material has been calculated in order to be tolerated later on. The position of the box inside the water tube is changing and therefore the pressure will change consequently. The *C-F* conversion characteristic of the capacitive interface oscillator is shown in Figure 17. The oscillator shows a response of 750 Hz/pF with only a

RESEARCH ARTICLE

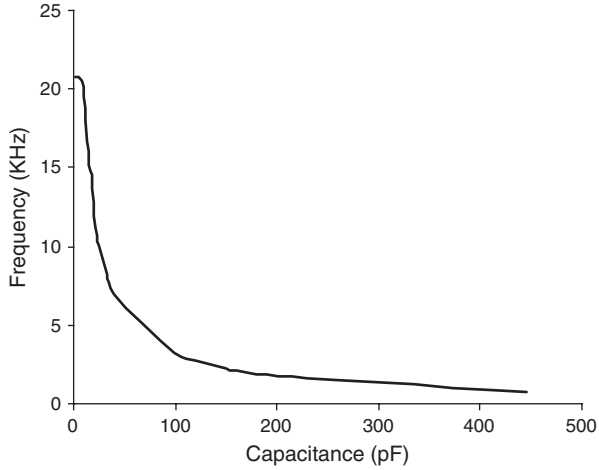

Fig. 17. *C-F* characteristics of the capacitive unit oscillator.

parasitic capacitance. The maximum difference between loading and unloading cycles was measured and expressed as a percentage of the full-scale deviation in order to calculate the hysteresis of the pressure sensor. In this work, the hysteresis was calculated to be 5% for the PE sensor as in Figure 18 which shows a better performance than the values calculated before for thick film devices.[41]

An external heating source has been used to change the water temperature from 0 to 80 °C. The thermal characteristic of the temperature sensor is shown in Figure 19. The characterization of the temperature sensors indicated a maximum sensitivity of 20 mV/°C with a base voltage

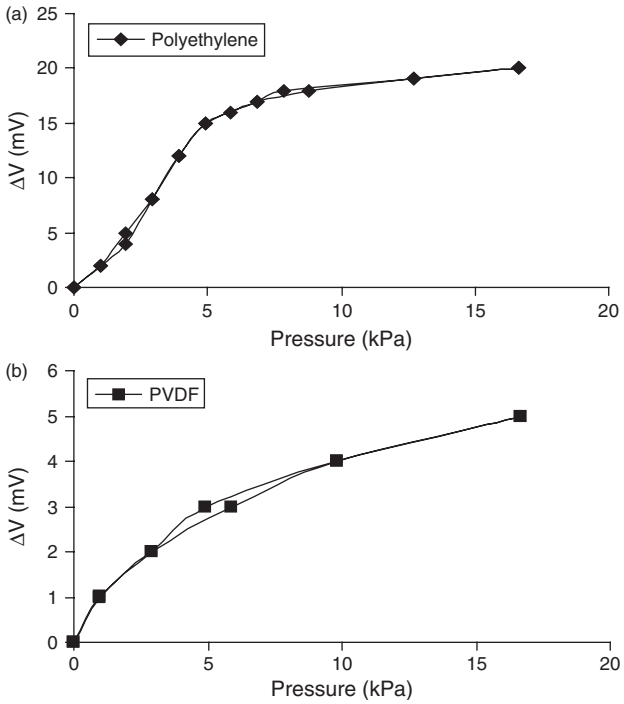

Fig. 18. Hysteresis of (a) the PE sensor and (b) the PVDF sensor as measured for one loading and unloading cycle.

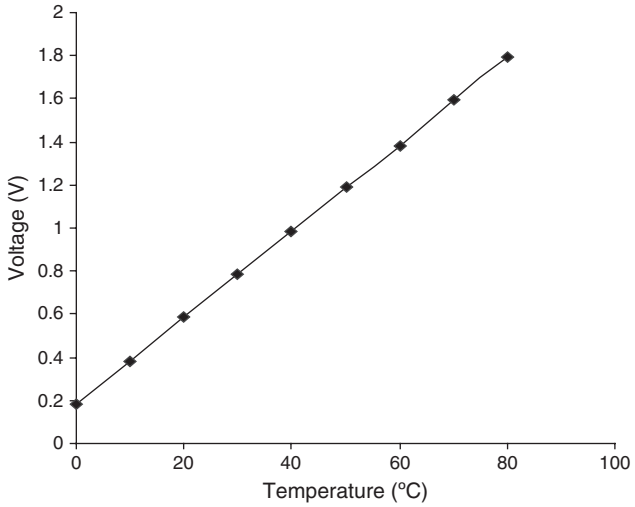

Fig. 19. Temperature sensitivity of the temperature sensor.

of 0.1 V. Obviously the resistive circuit performs well during the test range and configured to be used with any other sensor based on setting the reference, bias and gain resistors.

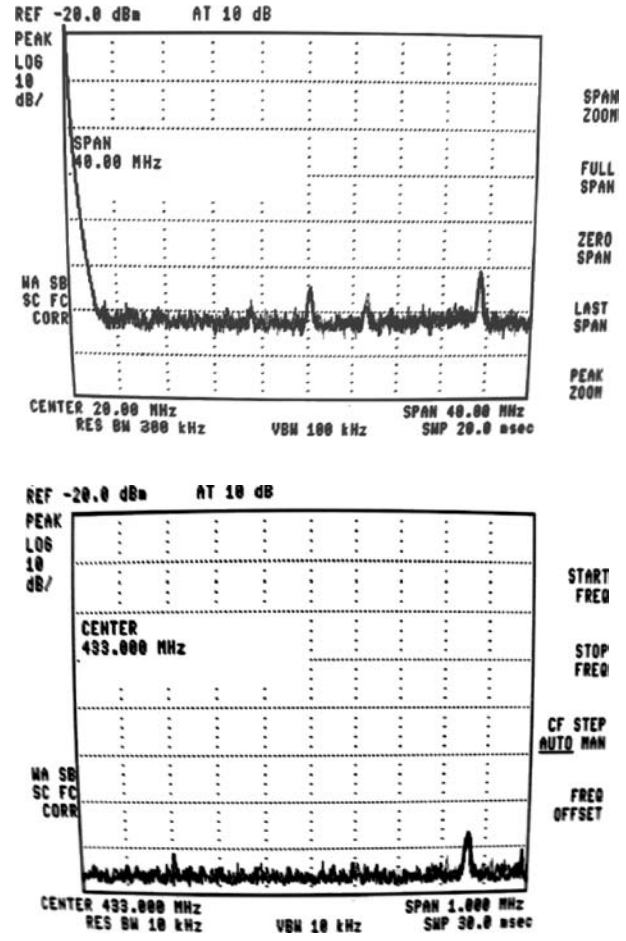

Fig. 20. Spectrum analyzer noise measuring of (a) Vcc-top mote board, (b) Capacitive sensor output-top mote board.

7.2. Noise Measurements

Noise can be a major issue in wireless systems involving high-speed processors and sensor conditioning interfaces. Any noise that carries over from the high-frequency components can alter the measurements being taken, and ruin the performance. To reduce some noise effects, grounding planes were used extensively, and the power units with conditioning interfaces were designed on boards separate from the processor and transceiver. Also, the board-to-board connectors were interlaced with grounds in order to further reduce the cross-board noise. As a result, noise was not a major issue when integrating the entire Mote together as expected. This section shows measurements taken using a Hewlett-Packard 8590L spectrum analyzer, to check if any high-frequency noise components can be observed in the power systems/conditioning interfaces.

Figure 20(a) shows a small noise spike in the top Mote board's V_{CC} at around 433.35 MHz. This noise was not found to affect the measurements or circuitry to any detrimental effect. The spectral analysis of the top board's GND displayed a similar result which displays the effect of the RF modules. The resistive and capacitive interface outputs were also measured for noise. Again both units presented very little noise at the output as in Figure 20(b) for the capacitive sensor.

8. PERFORMANCE ANALYSIS

This section evaluates our developed system in comparison with other motes that are similarly classified. Issues such as construction, communication and power management are discussed. Table V shows the overall comparison of the electrical and RF specifications. The Tyndall mote has been developed and used recently by many research institutes in Ireland.[8] Researchers at Berkeley developed the Mica mote platforms,[42] a series of programmable sensor motes commercially available from Crossbow technology.[43] Intel also has publicized the aptly called iMote.[44] Telos is another mote that developed by a research group in UC Berkley and presented in Ref. [45].

For our system, we chose PIC18F452 which met all the design requirements and has enough RAM and flash memory sizes. A larger flash storage, although useful for large applications, has not been the limiting factor in developing our WSN system.

The table shows that PIC18F452 has low measured power consumption in sleep and active modes in comparison with Tyndall and Mica2 motes. The microcontroller operated down to 2.0 V where the Atmega128 MCU (Mica family) will only run down to 2.7 V. The transition time from standby to active mode is no more than 4 μs where ATMega128 needs 4 ms to wakeup the system using external crystal and MSP430 needs 6 μs. It is worth to mention that MSP430 has Direct Memory Access (DMA) which reduce the load from MCU core, lower power consumption and increase the performance.

For communications the Nordic transceiver used in the Tyndall module boasts the highest data rate. The CC1000 has the lowest transmit and receive current. The data rate is reasonable since it is designed originally for low sampling rate based on the nature of both pressure and temperature changes. The power consumption figures given in Table V for the iMote are based on the Zeevo TC2000 chip used.[46] The mote power consumption figures of the TC2000 are considerably high. This is perhaps due to the use of a Bluetooth scheme designed for applications such

RESEARCH ARTICLE

Table V. Comparison between our mote and other developed motes.

Mote type	Our mote (2006)	Tyndall (2005)	Intel® mote (2005)	Telos (2004)	Mica 2 (2002)
Microcontroller					
Type	PIC18F452	ATMegal128	Zeevo TC2001	TI MSP430	ATMegal128
RAM (KB)	16	4	64	2	4
Flash (KB)	32	128	512	48	128
ADC channels	8	8		8	8
ADC resolution	10 bits	10 bits		10 bits	10 bits
Active power (mW)	8	16.5	195	3	33
Sleep power (μW)	40	45		6	180
Communication					
Type	CC1000	nRF2401	Blutooth	CC2420	CC1000
Data rate (bps)	38.4 K	1 M	723.2 K	250	38.4 K
Radio freq (Hz)	433/868/916 M	2.4 G	2.4 G	2.4 G	433/868/916 M
Transmit current	10	10.5	37.5	25	10
Receive current	8	18	34	27	8
Modulation type	FSK	GFSK		O-QPSK	FSK
Range	300 m	10 m	30 m	50–125 m	300 m
Power features					
Min operation (V)	3	3	3	1.8	2.7
Power mang modes	Ext wakeup/ sleep mode	Int sleep mode	Int sleep mode	Wakeup/ sleep mode	sleep
Receiver backup	Yes	No	No	No	No

as streaming audio as compared with sending intermittent packets of sensor data.

The CC1000 uses simple FSK modulation type and can be programmed to operate in any of three ISM bands. The Gaussian Frequency Shift keying (GFSK) adopted by the nrf2401 in a more bandwidth effective transmission-link compared with ordinary FSK modulation. The transmission range achieved with CC1000 is the highest (300 m) compared with the others. The helical design has been chosen for the antenna based on both size and range requirements. The whip antenna attachment of Mica2 motes adds to the overall size of the motes but has the advantage of extended range. The compact short range of Tyndall and iMote sensor nodes would perhaps more suited to indoor applications such as home automation. On the other hand, bigger long range might be better deployed outdoors for environmental applications as with our motes, Mica2 and Telos.

The main point to differentiate between our mote and the others is power management system of both the mote and the Base Station. All the sensor interface units of the mote can switched on/off under the control of the Base Station. Each mote can not initiate transmission unless receive command from the Base Station to avoid data collision. In addition a simple wakeup circuit has been designed and used with the capacitive circuitry to wakeup the processor from the sleep mode when there is a big change that exceeds a certain threshold. The CC1000 transceiver also supports a sleep mode and stays power down when it is not transmitting or receiving to minimize current consumption. The Base Station also provided with a developed backup circuit to provide an alternative battery supply in case the original firm supply went down for any reason. Such feature is so useful especially when the Base Station is placed in harsh environment to guarantee a continuous voltage supply for longer time periods. Telos mote has a similar feature to be in a sleep mode when there is no active processing but without remote control. The Tyndall module is characterized by using Field Programmable Gate Array (FPGA) device for signal processing uses. The main drawback with this technology is its power consumption. FPGA technology is SRAM based and therefore has relatively high power consumption in comparison to microcontroller technology.

9. CONCLUSION

This paper describes the design and implementation of wireless system suitable for environmental monitoring. Measuring the water pressure and temperature signals was the main scope of the work. The system reads data from two types of sensors, resistive (temperature) and capacitive (pressure). Anderson circuit configuration has been used efficiently for the resistive sensor, since it offers linear like behaviour. New features have been added to the design to improve the stability of the excitation current and make the circuit configurable for different sensor values. The capacitive interface is based on capacitance-frequency-voltage conversion that uses PLL to convert the frequency to voltage. The PLL unit has 1% linearity and consumes a low power.

The pressure sensing properties of sandwich capacitors based on PE and PVDF were evaluated using the specially constructed wireless data acquisition system for the capacitive interface. It was seen that each material displayed a high sensitivity to pressure changes in the range 0–17 kPa. It was found that the PE sensors were the most sensitive, but each device displayed low hysteresis and repeatability. It can be concluded that PE is the most sensitive to pressures over a small range; however PVDF could find applications in systems where pressures measurements over a large range are required Two mechanisms have been adopted to reduce further the overall power consumption. These are power scheduling and wakeup circuit for the capacitive interface. The first one is implemented fully by the MCU in order to switch on/off all the system units.

A wakeup circuit has been designed to interrupt the MCU when it is in the sleep mode and the capacitive samples are changing significantly. It was found that such design is more suited for the capacitive interface than the resistive one where the circuit consumes much less power even if it is kept working continuously. The performance of the mote sensor has been verified in terms of power figures.

A novel wireless protocol has been adopted to configure the mote units and control the communication traffic between the nodes and Base Station. A backup circuitry has been designed for the hard conditions operation to provide alternative power supply to the Base Station.

Acknowledgments: This research was supported by the Enterprise Ireland Commercialization Fund 2003, under the technology development phase, as part of the MIAPS project, reference no. CFTD/03/425.

References and Notes

1. T. Akin, K. Najafi, and R. Bradley, *IEEE J. Solid-State Circuits* 33, 109 **(1998)**.
2. P.-J. Chen, D. C. Rodger, S. Saati, M. S. Humayun, and T. Yu-Chong, *IEEE 21st International Conference on Micro Electro Mechanical Systems (MEMS)* **(2008)** pp. 58.
3. E. Johannessen, L. Wang, C. Wyse, D. Cumming, and J. Cooper, *IEEE Biomedical Engineering* 53, 2333 **(2006)**.
4. L. Wang, T. D. Drysdale, and D. R. S. Cumming, *IEEE Transactions on Biomedical Engineering* 54, 2020 **(2007)**.
5. C. A. Grimes, M. K. Jain, R. S. Singh, Q. Cai, A. Mason, K. Takahata, and Y. Gianchandani, *Proc. 14th IEEE conf. Micro electro mechanical systems* **(2000)** pp. 278.
6. Y. Navid, M. Andraw, K. Najafi, and W. Kensall, *Sens. Actuators* 84, 351 **(2000)**.
7. K. L. Kraver, R. G. Matthew, S. D. Timothy, B. L. Peter, C. Geun Sig, H. Wolfang, and B. B. Richard, *Sens. Actuators* 91, 266 **(2001)**.
8. S. Bellis, K. Delaney, B. O'Flynn, J. Barton, K. Razeeb, and C. O'Mathuna, *Computer Commutations* 28, 1531 **(2005)**.

9. Y. K. Seok, G. Joonho, K. Jinbong, K. Hong-Jeong, K. Kyunghyun, P. Daesik, K. Myeung su, S. Hyungcheol, L. Kwyro, K. Juhyoun, and Y. Euisik, *Sens. Actuators* 102, 27 **(2004)**.

10. A. DeHannis and K. Wise, *IEEE Microelectromechanical Systems* 14, 12 **(2005)**.

11. A. Mohan, A. P. Malshe, S. Aravamudhan, and S. Bhansali, *Proc. 54th conf. IEEE Electronic Components and Technology Conference* **(2004)** Vol. 1, pp. 948.

12. S. Anumalla, B. Ramamurthy, D. C. Gosselin, and M. Burbach, *IEEE Conf. Electro Information Technology* **(2005)**.

13. E. Johannessen, W. Lei, C. Li, T. T. Boon, A. Mansour, A. Alexander, R. W. J. Stuart, Y. S. Philippa, M. F. Alan, F. W. Brian, B. P. Steve, C. R. S. David, and C. M. Jonathan, *IEEE Trans. Biomedical Engineering* 51, 525 **(2004)**.

14. K. Arshak and E. Jafer, *Proc. IEEE Conf. Sensors*, CA (USA) **(2005)**.

15. R. Puers, *J. Micromech. Microeng.* 9 **(1999)**.

16. T. Farnham, *Proc. IEEE 6th Conf. Universal Personal Communications* **(1997)** Vol. 2, pp. 918.

17. K. Arshak, D. Morris, A. Arshak, O. Korostynska, E. Jafer, D. Waldron, and J. Harris, *Biomol. Eng.* 23, 253 **(2006)**.

18. K. Arshak, A. Arshak, D. Morris, O. Korostynska, and E. Jafer, *IEEE Sens. J.* 7, 122 **(2007)**.

19. R. Puers, *Sensor and Actuators* 37–38 **(1993)**.

20. P. A. Payne and Q. X. Chen, *IEE Colloquium on Physiological Pressure Measurement* 7/1 **(1990)**.

21. Measurement Specialities, Piezo Film Sensors: Technical Manual, Norristown **(1999)**, p. 86.

22. P. A. Payne, Q. X. Chen, F. Moss, R. E. Banks, and S. Smith, *IEE Colloquium on Molecular Electronics* 6/1 **(1990)**.

23. F. Bauer, *ISE 10. Proceedings. 10th International Symposium on Electrets* **(1999)** pp. 647.

24. J. Dargahi, M. Parameswaran, and S. Payandeh, *Int. Conference on Intelligent Robots and Systems*, Victoria, B.C., Canada **(1998)**.

25. G. Harsanyi, Polymer Films in Sensor Applications: Technology, Materials, Devices and their Characteristics, Technomic Publishing Co. Inc., **(1995)**.

26. S. C. Domenech, V. L. S. Severgnini, E. A. Pinheiro, A. O. V. Avila, N. G. Borges, E. Lima, V. Drago, and V. Soldi, *Polymer Degradation and Stability* 88, 461 **(2005)**.

27. M. Paajanen, J. Lekkala, and K. Kirjavainen, *Sens. Actuators A: Physical* 84, 95 **(2000)**.

28. K. Arshak, E. Jafer, and A. Fox, *Compos. Sci. Technol.* 65, 757 **(2005)**.

29. Dual CMOS Timer, Manual Sheet, Texas Instruments.

30. A. Arshak, K. Arshak, D. Morris, O. Korostynska, and E. Jafer, *Sens. Actuators* 122, 242 **(2005)**.

31. K. I. Arshak, A. K. Ray, C. A. Hogarth, D. G. Collins, and F. Ansari, *Sens. Actuators A: Physical* 49, 41 **(1995)**.

32. PIC family Microcontrollers: www.microchip.com.

33. CC1000 Chipcon RF Transceiver data sheet: http://www.chipcon.com.

34. M. Sgroi, J. L. da Silva, F. De Bernardinis, F. Burghardt, A. Sangiovanni-Vincentelli, and J. Rabaey, *IEEE Proc. ICASSP* 6, 3726 **(2000)**.

35. W. B. Heinzelman, A. P. Chandrakasan, and H. Balakrishnan, *IEEE Trans Wireless communications* 1, 660 **(2002)**.

36. K. F. Anderson, *IEEE Instrumentation and Measurement Magazine* 1, 5 **(1998)**.

37. K. Arshak, E. Jafer, J. Orr, A. Arshak, D. Morris, D. McDonagh, J. D. Quartararo, H. Dämpfling, and C. Y. Huang, *Transactions on Systems, Signals and Devices (Issues on Sensors, Circuits & Instrumentation Systems)*, Vol. 2, No. 4, 2006–2007.

38. Universal Capacitive Readout IC (MS3110) manual sheet, Irvine Sensors.

39. TPS72 Micropower Voltage regulator, manual sheet, Texas Instruments: http://focus-webapps.ti.com.

40. ASM121 Ultra Low Power Temperature Sensor, data sheet: http://www.andigilog.com/.

41. K. I. Arshak, D. McDonagh, and M. A. Durcan, *Sens. Actuators* 79, 102 **(2000)**.

42. J. Hill and D. Culler, *IEEE Micro.* 22, 12 **(2002)**.

43. Crossbow Technology Inc., Website: http://www.xbow.com.

44. Intel Mote overview webpage: http://www.intel.com/research/exploratory/motes.htm.

45. J. Polastre, R. Szewczyk, and D. Culler, *Proc. IEEE 4th Conf. Information Processing in Sensor Networks* **(2005)** pp. 364.

46. TC2000 Single Chip Bluetooth Solution Pre-Production Data Sheet, MK-0004 Version 2.9006v16, October **(2002)**.